Numerical Calculation of High Pressure Compaction for Porous Materials

높은 압력을 받는 다공질재료의 압축에 대한 수치해석적 연구

Park, Jong-Kwan
朴 鍾 寬

要 旨

높은 압력을 받는 다공질 재료의 압축에 대한 이론적 응력-변형의 구성 방정식이 제안되었다. 본 구성 방정식에는 소성이론을 근거로하여 하나의 yield function과 nomality rule이 적용되고 공극율(porosity)을 strain-hardening parameter로 사용하고 있다. 위 구성 방정식은 유한요소법을 이용한 2차원의 콤퓨터 프로그램에 삽입되어 다공질재료의 압축을 수치해석적으로 연구하는데 쓰였다. 특히 다공질 재료의 압축과 관련되어 발생되는 여러가지 현상을 규명하는데 수치해석적 연구의 중요성이 인식되고 하중제거후에 압축된 재료에 발생되는 인장응력과 균열에 관한 현상을 고찰하였다.

Abstract

A practical constitutive equation with sufficient generality is proposed for porous materials to deal with plastic pore compaction and pore related strain-hardening. With an application of this proposed model, finite element calculations are executed for the compaction of a porous material. Results show powerful potential of finite element method in a quantitative investigation of the process of the compaction. Special attention is given to the process of unloading during which the development of tensile principal stress may lead to phenomena such as lamination and end-capping.

1. Introduction

Porous material includes many kinds of materials such as soils, rocks, concretes, ceramics, and metallic powders. These materials have been interested in military and industrial applications because of their mechanical properties of shock isolation and attenuation[1~2]. Theoretical approach to describe the mechanical behaviors of the materials involves a constitutive modelling. There have been developed many constitutive models for soils and they are mostly applied for the studies of geotechnical engineering. They are mostly based upon continuum plasticity theory and the assumption of incompressibility of granular particles. Under the high pressure, however,

* 正會員, 경기공업개방대학 조교수

these materials undertakes very large complex deformation. The deformation of the material is considered to occur due to the pore collapse and the compression of the soild component.

Perhaps the most widely used constitutive model of porous material under high pressure has been known for the phenomenological Pressure-α model of Herrmann[3]. In this model, a constitutive equation for a porous material is derived from the equation of state of solid component, plus porosity which varies the state of stress in the material. Recently, Swegle[1] suggested a constitutive model for porous materials based upon the extension of Herrmann's Pressure-α model. This extension is physically motivated to describe the shear enhanced pore compaction of the porous material. In this study, a constitutive model is proposed with the further extension of Swegle's model for describing the behavior of a porous material under high pressure and the model is applied to the finite element analysis of compaction of a powder material.

For the application of the proposed model, an elasto-plastic finite element calculation is executed for the die compaction of powder. Die compaction is a fabrication process for producing powder compacts under high pressure. As an adventage of this method is its ability to produce variously shaped powder products with speed. However, there are well recognized problems, heterogeneous density distribution and fracturing during unloading. The numerical analysis of die compaction consists of two parts: loading and unloading. The loading is executed by incrementally increasing a prescribed punch displacement. Unloading is executed by incrementally decreasing the surface tractions developed during loading. On the basis of the contact node algorithm of Hehenbergen [11], the finite element code is implemented to deal with the little studied problem of powder friction. Resulting density and stress distributions in cyrindical compacts are discussed for the different degrees of wall friction. Particularly, residual tensile principal stresses and radial stresses are studied to understand the end-capping problem associated with unloading[4].

2. Constitutive Model

Carroll and Holt's pressure-α relation[5] is applied for the entire porous body. If the material is saturated with fluid, the relation between externally applied pressure P and pressure P_s in the solid component can be written by

$$VP=V_sP_s+V_fP_f, \tag{1}$$

$$P=\alpha P_s+\eta P_f, \tag{2}$$

or where V, V_s, and V_f are the volume of total material, solid compnent, and fluid, respectively. The parameter α is defined as the specific solid volume fraction V_s/V $(=1-\eta)$, and porosity η is the ratio of V_f/V. For the dry material P_f is regarded as zero. Then the $P-\alpha$ relation become simply

$$P=\alpha P_s \tag{3}$$

This is an exact result, independent of the material law and loading path.

The Mie-Grueisen equation is often used for representing the volumetric response equation of solid under hyrostatic pressure. The equation is

$$P=A(V_{s0}/V_s-1)+B(V_{s0}/V_s-1)^2+C_s(V_{s0}/V_s-1)^3+DEV_{s0}/V_s, \tag{4}$$

where A, B, C, and D are constants, V_{s0} is the initial volume of solid, V_s is the current volume of solid after deformation, and E is the specific internal energy per unit mass.

Elastic response

The elastic response of homogeneous and isotropic material is described by Hook's law. Pressure and deviatoric stress increments are expressed in terms of elastic volumetric strain $d\varepsilon_{kk}^e$ and deviatric strains de_{ij}^e

$$dP=Kd\varepsilon_{kk}^e \tag{5}$$

$$dS_{ij}=2Gde_{ij}^e \tag{6}$$

where K and G are the bulk and the shear modulus of the material. These values, K and G, are usually obtained to be constants from the experimental testing. However, the elastic modulus of the porous material can not be considered as constants under the high pressure. As an advantage of this model, the values of K and G can be evaluated through this modelling.

One of the experimental expression of elastic pressure is written by sound velocity measurements and the parameter α,

$$(d\alpha/dP)\ \text{elastic}=(1/h^2(\alpha)-1)/K_{s0}, \tag{7}$$

$$\text{where } h(\alpha)=1+(1-\alpha)(C_0/C_{s0}-1)/(1+\alpha), \tag{8}$$

K_{s0}=solid bulk modulus at zero pressure,

C_0, C_{s0}=sound velocity at zero pressure.

This expression can be written simply by

$$dP^e=K_\alpha d\alpha^e \tag{9}$$

The pressure-α relation of Eq. (3) is true for any stage of pressure, so the pressure increment dP^e can be expressed by

$$dP^e=df_p^e(\alpha, V)=\frac{\partial f_p(\alpha, V)}{\partial V}d\alpha^e+\frac{\partial f_p(\alpha, V)}{\partial V}Vd\varepsilon_{kk}^e \tag{10}$$

From Eq. (5) and (10), the bulk modulus K is defined by

$$K=-K_\alpha V\frac{\partial f_p(\alpha, V)}{\partial V}\Big/\left(K_\alpha-\frac{\partial f_p(\alpha, V)}{\partial \alpha}\right) \tag{11}$$

Determination of the shear modulus G involves two assumptions that

$$dS_{ij}=\alpha\, dS_{ijs} \tag{12}$$

$$\frac{d\varepsilon^e_{ijs}}{d\varepsilon_{ij}^e}=\frac{-dV_s^e/V_s}{-dV^e/V}=\frac{d\varepsilon^e_{kks}}{d\varepsilon_{kk}^e}=\frac{de^e_{ijs}}{de^e_{ij}} \tag{13}$$

From these assumptions the shear modulus G can be defined by

$$G=\frac{dV_s^e}{dV^e}G_s \tag{14}$$

where G_s is the shear modulus of the solid material.

Plastic response

First, we list several basic equations to be used in this formulation :

Yield function

$$g(J_1, \sqrt{J_2'}, \alpha)=0, \tag{15}$$

Strain increment in the plastic region

$$d\varepsilon_{ij}=d\varepsilon_{ij}^e+d\varepsilon_{ij}^p, \tag{16}$$

Associated flow rule

$$d\varepsilon_{ij}^p=d\lambda\frac{\partial g}{\partial \sigma_{ij}}, \tag{17}$$

Increment of stress components

$$dP=Kd\varepsilon_{kk}^{e}=K(d\varepsilon_{kk}-d\varepsilon_{kk}^{p}), \tag{18}$$

$$dS_{ij}=2Gde_{ij}^{e}=2G(de_{ij}-de_{ij}^{p}), \tag{19}$$

The plastic volumetrie strain increment $d\varepsilon_{kk}^{p}$ and the deviatoric strain increment de_{ij}^{p} are derived from Eq. (17) in terms of the invariants J_1 and $\sqrt{J_2'}$:

$$d\varepsilon_{kk}^{p}=d\varepsilon_{11}^{p}+d\varepsilon_{22}^{p}+d\varepsilon_{33}^{p}=3d\lambda\frac{\partial g}{\partial J_1}, \tag{20}$$

$$de_{ij}^{p}=d\varepsilon_{ij}^{p}-\frac{1}{3}d\varepsilon_{kk}^{p}\delta_{ij}=d\lambda\frac{S_{ij}}{2\sqrt{J_2'}}\frac{\partial g}{\partial\sqrt{J_2'}} \tag{21}$$

Then, Eqs. (18) and (19) can be written as

$$dP=K\,d\varepsilon_{kk}-3K\,d\lambda\frac{\partial g}{\partial J_1}, \tag{22}$$

$$dS_{ij}=2G\,de_{ij}-G\,d\lambda\frac{S_{ij}}{\sqrt{J_2'}}\frac{\partial g}{\partial\sqrt{J_2'}} \tag{23}$$

The scalar quantity $d\lambda$ is derived from the assumption that any increment of the yield function should always be kept at zero in the plastic region:

$$dg=\frac{\partial g}{\partial J_1}dJ_1+\frac{\partial g}{\partial\sqrt{J_2'}}d\sqrt{J_2'}+\frac{\partial g}{\partial\alpha}d\alpha=0, \tag{24}$$

$$dJ_1=3P=3\,K\,d\varepsilon_{kk}-9K\,d\lambda\frac{\partial g}{\partial J_1}, \tag{25}$$

$$d\sqrt{J_2'}=\frac{(S_{ij}dS_{ij})}{2\sqrt{J_2'}}=\frac{G(S_{ij}de_{ij})}{\sqrt{J_2'}}-G\,d\lambda\frac{\partial g}{\partial\sqrt{J_2'}} \tag{26}$$

Additionally, we can obtain $d\alpha$ from the $P-\alpha$ equation:

$$f_p(\alpha, V)=\alpha P_s, \tag{27}$$

$$df_p=\frac{\partial f_p}{\partial\alpha}d\alpha+\frac{\partial f_p}{\partial V}dV, \tag{28}$$

$$d\alpha=\left[df_p+V\frac{\partial f_p}{\partial V}d\varepsilon_{kk}\right]\Big/\frac{\partial f_p}{\partial\alpha} \tag{29}$$

From the condition that the increment of the pressure df_p in Eq. (28) must equal the increment of the pressure dP in Eq. (22), $d\alpha$ can be derived as

$$d\alpha=\left[\left(K+V\frac{\partial f_p}{\partial V}\right)d\varepsilon_{kk}-3\,K\,d\lambda\frac{\partial g}{\partial J_1}\right]\Big/\frac{\partial f_p}{\partial\alpha} \tag{30}$$

Substituting Eqs. (25), (26) and (30) into Eq. (24), we find

$$d\lambda=\frac{1}{H}\left[3K\frac{\partial g}{\partial J_1}d\varepsilon_{kk}+\frac{G(S_{ij}de_{ij})}{\sqrt{J_2'}}\frac{\partial g}{\partial\sqrt{J_2'}}+\left(K+V\frac{\partial f_p}{\partial V}\right)\frac{\partial g}{\partial\alpha}d\varepsilon_{kk}\Big/\frac{\partial f_p}{\partial\alpha}\right], \tag{31}$$

$$\text{where } H=9K\left(\frac{\partial g}{\partial J_1}\right)^2+G\left(\frac{\partial g}{\partial\sqrt{J_2'}}\right)^2-3K\frac{\partial g}{\partial J_1}\Big)^2\Big/\frac{\partial f_p}{\partial\alpha} \tag{32}$$

Now, combining Eqs. (22) and (23), we obtain the stress and strain relations:

$$\begin{aligned}d\sigma_{ij}&=dP\delta_{ij}+dS_{ij}\\&=\left(K\,d\varepsilon_{kk}-3K\,d\lambda\frac{\partial g}{\partial J_1}\right)\delta_{ij}+2Gde_{ij}-d\lambda\frac{GS_{ij}}{\sqrt{J_2'}}\frac{\partial g}{\partial\sqrt{J_2'}}\\&=\left[\left(K-\frac{2}{3}G\right)\delta_{ij}-C_1\delta_{ij}-C_2S_{ij}\right]d\varepsilon_{kk}\\&\quad-(C_3\delta_{ij}+C_4S_{ij})(S_{ij}d\varepsilon_{ij})+2Gd\varepsilon_{ij},\end{aligned} \tag{33}$$

$$C_1=\frac{1}{H}\left[3K\frac{\partial g}{\partial J_1}+\left(K+V\frac{\partial f_p}{\partial V}\right)\frac{\partial g}{\partial\alpha}\Big/\frac{\partial f_p}{\partial\alpha}\right], \tag{34}$$

$$C_2=-\frac{1}{H}\left[\frac{G}{\sqrt{J_2'}}\frac{\partial g}{\partial\sqrt{J_2'}}\left(3K\frac{\partial g}{\partial J_1}+\left(K+V\frac{\partial f_p}{\partial V}\right)\frac{\partial g}{\partial\alpha}\Big/\frac{\partial f_p}{\partial\alpha}\right)\right], \tag{35}$$

$$C_3=-\frac{1}{H}\left(3K\frac{\partial g}{\partial J_1}\right)\left(\frac{G}{\sqrt{J_2'}}\frac{\partial g}{\partial\sqrt{J_2'}}\right), \tag{36}$$

$$C_4=-\frac{1}{H}\left(\frac{G}{\sqrt{J_2'}}\frac{\partial g}{\partial\sqrt{J_2'}}\right)^2 \tag{37}$$

When C_1, C_2, C_3, and C_4 are zero, the constitutive equation becomes that of the elastic region. For the case of unloading, elastic unloading is assumed.

3. Applications

The elasto-plastic finite element calculations are performed for the compaction of metal and ceramic powders in a rigid cylindrical die. Ralatively few experimental data are available to determine the material parameters of powder materials. As an example of metal powder, aluminum powder was examined. The parameters for the aluminum powder were obtained from the experimetal data of 22% porous aluminum studied by Johnson[6] and Swegle[1]. As an example of ceramic powder, an artificial ceramic powder was constructed using the experimental data for sand. The selection of these powders seems to be appropriate for investigating general features of the die compaction of powder materials.

Material parameters based on 22% porous 2024 aluminum[1,3]:

Initial porosity $(\eta_0)=22\%$,

Density of the solid $(\rho_s)=2.7\text{g/cm}^3$,

Shear modulus of the solid $(G_s)=27.4$ GPa,

Bulk modulus of the solid $(K_{s0})=78.2$ GPa,

Ratio of the bulk sound velocity to the solid sound velocity $(C_0/C_{s0})=0.528$,

The pressure-volume equation for the solid,

$$P_s=78.2(V_{s0}/V_s-1)+172(V_{s0}/V_s-1)^2+40(V_{s0}/V_s-1)^3 \text{ in GPa.} \tag{38}$$

An elliptical yield function[1] was used for the yield criterion of the alumium powder. The parameters were determined from uniaxial strain compression data[6]. The function is given by

$$[P/P_1(\alpha)]^2+[\sqrt{3J_2'}/Y_1(\alpha)]^2+1=0, \tag{39}$$

where $P_1(\alpha)$ and $Y_1(\alpha)$ are expressed by cubic spline functions,

$$f_i=A_i+B_i(\alpha-\alpha_i)+C_i(\alpha-\alpha_i)^2+D_i(\alpha-\alpha_i)^3,\quad \alpha<\alpha<\alpha_{i+1}, \tag{40}$$

for $P_1(\alpha)$,

$\alpha_1=0.77823$, $\alpha_2=0.96158$,

$A_1=0.06033$, $A_2=0.36356$,

$B_1=1.69858$, $B_2=3.26318$,

$C_1=-9.26564$, $C_2=17.779$,

$D_1=49.2034$, $D_2=8441.51$,

(A_i, B_i, C_i, and D_i are given in GPa).

For this aluminum powder no attempt was made to interpret the function $P_1(\alpha)$ using the spherical collapse model[5]. A polynomial function was used for the spline function $Y_1(\alpha)$:

$$Y_1(\alpha)=Q_0(1-\alpha)^m P_1(\alpha), \tag{41}$$

where $Q_1=1.00$, $m_1=0.0$, $P<0.1$ GPa

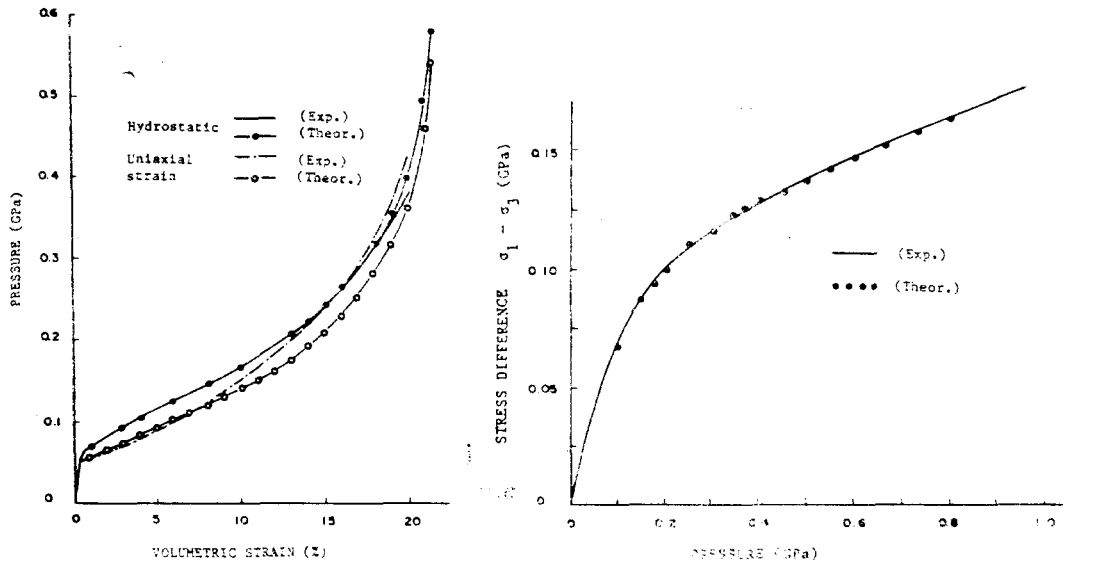

(a) Hydrostatic and uniaxial strain loading

(b) Stress difference as a function of pressure at uniaxial strain condition.

Fig. 1. Model calculations for 22% porous aluminum.

$Q_2=1.45$, $m_2=0.21$, $P>0.1$GPa.

Calculated pressure-volume and stress difference ($\sigma_1-\sigma_3$) pressure relationships are shown in Fig. 1 (a) and 1 (b), respectively. The calculation, obtained using Swegle's original yield function, did not reproduce the experimental pressure-deviatoric stress invariant curve well, This disagreement motivated us to modify Swegle's material constants to the data shown above. Detailed discussions of the uniaxial strain compression can be found in Reference[7].

Material parameters based on Ottawa sand :

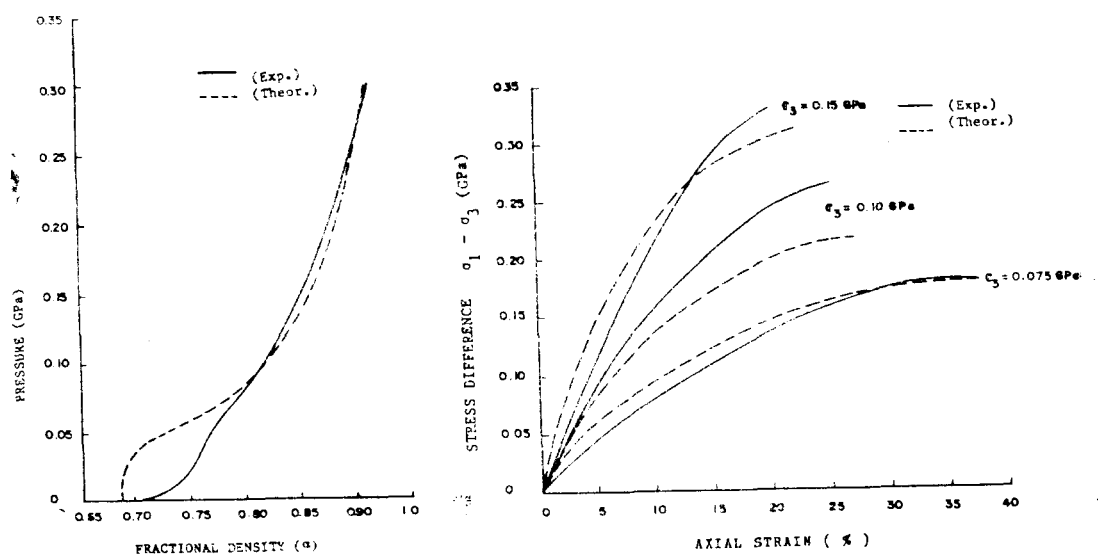

(a) Hydrostatic pressure

(b) Triaxial compressioin

Fig. 2. Model Calculations for Ottawa sand

Initial porosity $(\eta_0)=31\%$,

Specific density of the solid $(\rho_s)=2.7\ \mathrm{g/cm^3}$,

Shear modulus of the solid $(G_s)=15.0$ GPa,

Bulk modulus of the solid $(K_{s0})=25.0$ GPa,

Ratio of the bulk sound velocity to the solid sound velocity $(C_0/C_{s0})=0.528$,

The pressure-volume equation for the solid,

$$P_s=25(V_{s0}/V_s-1)+60.3(V_{s0}/V_s-1)^2 \text{ in GPa.} \tag{42}$$

An attempt was made to interpret the pressure fuction $P_1(\alpha)$ utilizing a spherical collapse model. The function $P_1(\alpha)$ is given by

$$P_1(\alpha)=\frac{Y}{\beta}[(1-\alpha)^{-2\beta/3}-1], \tag{43}$$

where $Y=0.0175$ GPa,

$\beta=2.322$.

Figure 2(a) shows the numerically generated pressure-α relations and the experimental data for Ottawa sand[8]. The discrepancy in the range of pressure below 0.08 GPa was caused by the lack of elastic behavior in Ottawa sand and choice of $P_1(\alpha)$.

For the yield criterion of this ceramic powder, a lemniscate function was used. The parameters were determined from the high pressure triaxial compression data for sand[8]. This function is given by

$$g=[P+K(\alpha)]^2+(\sqrt{3J_2'})^2-B^2(\alpha)\cos^{2n}(\pi\theta/2\phi), \tag{44}$$

where

$$K(\alpha)=K_0+CP_1(\alpha), \tag{45}$$

$$B(\alpha)=P_1(\alpha)+K(\alpha), \tag{46}$$

$K_0=0.04$GPa,

$C=0.05$,

$\phi=60°$,

$n=0.3$.

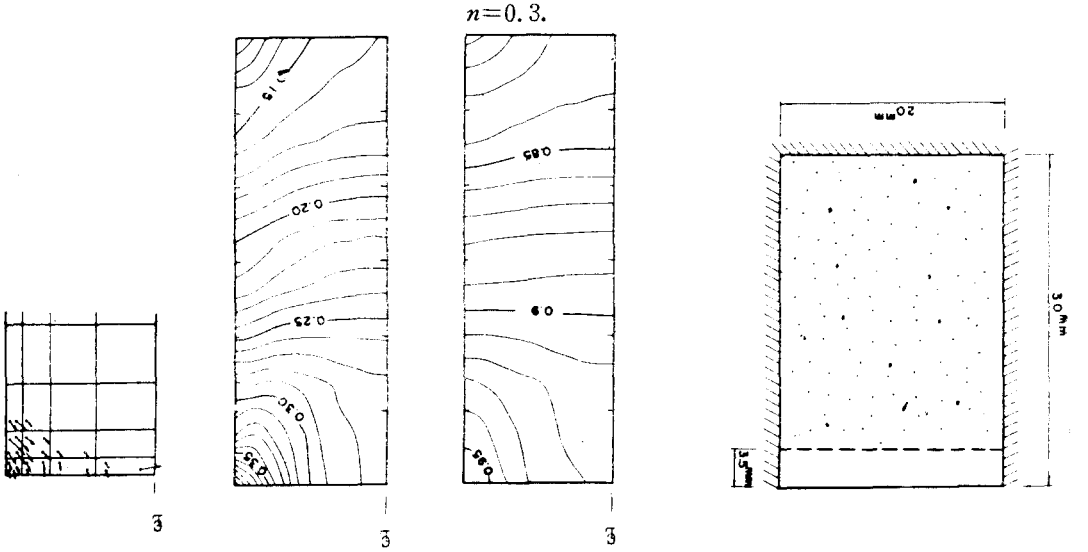

(a) Geometry (b) Fractional denesity (c) Axial stress (d) Tensile stresses after unloading

Fig. 3. Aluminum powder compaction

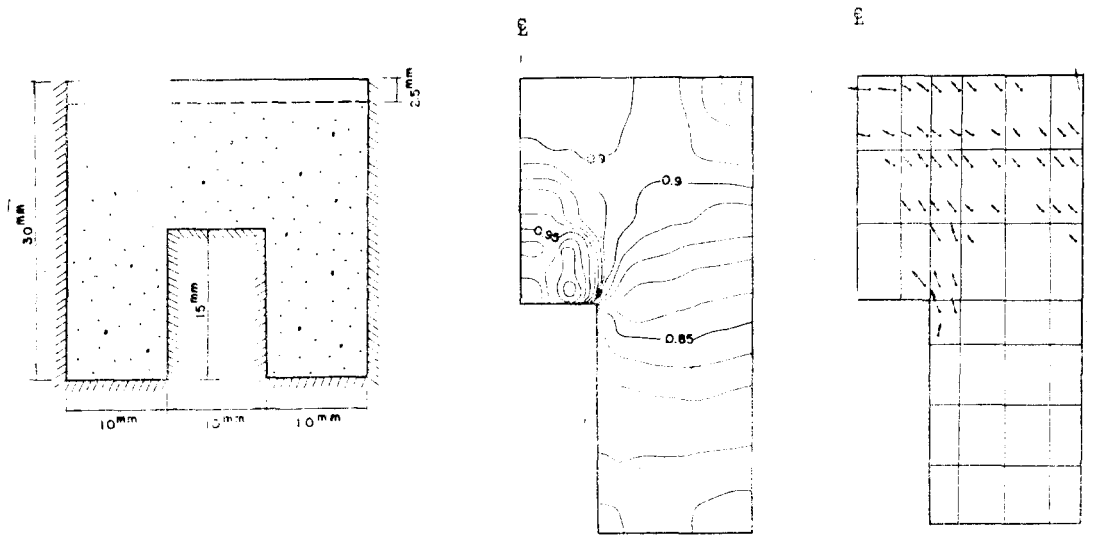

(a) Geometry (b) Fractioal density (c) Tensile stresses after unloading

Fig. 4. Aluminum powder compaction in a concentric die

Figure 2(b) shows a comparsion of the stress difference $(\sigma_1-\sigma_3)$ axial strain relation calculated by the model with the experimental data for Ottawa sand under the triaxial compression condition.

A simulation was carried out for the compaction of the aluminum powder in a cylindrical die of diameter 20 mm and height 30 mm. The maximum displacement of the upper punch was 3.5 mm. The right half of the cylinder was divided by 32 elements. Finer elements were used in the region close to the wall because of expected large shear deformations. The so-called contact node algorithm[11] was applied for the treatment of wall friction. The method is to consider the frictional boundary as a mixed condition. The frictional coefficient, the ratio of the tangential to nomal boundary traction, is prescribed on the frictional boundary, and displacement along the wall is allowed. The contours of the fractional density distribution and the axial stress for the frictional coefficient of 0.3 are shown in Fig. 3. The values of maximum around the upper right corner and the minimum around the lower right corner depend strongly upon the magnitude of the wall friction. In the case of no wall friction, the density and the stress in the compact have unique values and no variations appear. Unloading was simulated by incrementally releasing the surface boundary tractions developed during pressing. It is noted that the unloading was assumed to be elastic. The most significant result of the unloading was the build-up of tensile stress around the upper right surface of the compact associated with releasing the top surface tractions. Arrows in Fig. 3(d) indicate the magnitudes and the directions of the maximum principal tensile stresses.

For the application of a complex die, compaction of aluminum powder was simulated in a cylindrical die with concentric profile. Top punch displacement of 2.5 mm was applied. The resulting contour of fractional density distribution for the frictional coefficient of 0.3 and the bulit-up of residual tensile stresses are shown in Fig. 4. Some errors are involved in the density distribution especially in the region near internal edge because this finite element calculation

does not include the convection and rotation terms. However, the general aspects of this density distribution are consistent with the X-ray measurements of density variation in a similarly shaped die by Broese van Groenou et al.[9~10].

4. Summary and Conclusions

The elasto-plastic constitutive model was presented for the porous material. Important features of the proposed model are :

a. Overall stress components are described in terms of the porosity and the stress in solid.
b. Plasticity behavior is described by a conventional closed yield surface and an associated hardening flow rule.
c. Elastic material moduli are obtained from the elastic moduli of the solid.
d. Yield function parameters are determined by experimental test results as well as by a mechanistic modelling of pore compaction.

The proposed model was applied for the finite element calculation to investigate the compaction behaviors of powder materials. The mechanism of powder-wall friction was implemented into the finite element program by the contact node algorithm. This methed was easily applicable to the process of both loading and unloading. Some selected results of die compaction are :

1. Density and axial stress distributions were in good agreement with the results of Hehenberger [11~12] and Thompson [13]. Density distibution in a compact with a concentric profile was in good agreement with experimental results in the general aspect of density variation. This is the evedance that the proposed model is very effective for predicting the stress-strain behavior of powder under very high pressure.
2. Tensile zone was predicted in the upper portion of the cylindrical compact during unloading. A crack may develop along the direction of the principal tensile stress plane. So far as orientation is concerned, the direction of the crack was in good agreement with Thompson's experimental and finite element analyses of end-capping in pressed green compacts[14]. The szie of the tensile zone was directly related to the magnitude of coefficicent of wall friction.

Therefore, the unified finite element calculations of loading and unloading provide information necessary for calculation strngth and serviceability of the compact as well as for optimization of the compaction process.

Acknowledgements

This study is a part of author's Ph, D. dissertation at North Carolina State University. Deepest apppreciation is expressed to Professor Y. Horie, the chairman of advisory committee, for his guidance and support through the course of this study.

References

1. Swegle, J.W., "Constitutive Equation for Porous Materials with Strength," J. Appl. Phys., 51, 1980, pp. 2574~2580.
2. Park, J.K. and Horie, Y., "Constitutive Equation for Geological Materials under High Dynamc iLoading," Proc. of Second Symposium on the Interaction of Non-Nuclear Munitions with Structures,

Panama City, Florida, April, 1985, pp. 278~283.
3. Harrmann, W. "Constitutive Equation for the Dynamic Compression of Ductile Porous Materials," J. Appl. Phys., 40, 1969, pp. 2490~2499.
4. J-K Park, "Die Compaction of Powder: Constitutive Modelling and Finite Element Calculatiion," Ph. D. Dissertation, North Carolina State University, 1985.
5. Carroll, M.M., "Compression of Dry or Fluid Filled Porous Materials," J. of Eng. Mech. Div., ASCE, EM5, 1980, pp. 969~989.
6. Johnson, J.N. and Green, S.J., "The Mechanical Response of Porous Media Subject to Static Loads," in The Effects of Voids on Material Deformation, Cowin, S.C. and Carroll, M.M. Ed., The Appl. Mech. Div., ASME, AMD 16, 1976, pp. 93~123.
7. Horie, Y., Park, J.K., Hoy, D.E.P., and Whitfield, J.K., "High Pressure Equation of State for Metal Ceramic Powders," Final Report Part 1, 2, Under a Project Entitled ''Support of Darpa Program in Dynamic Synthesis of Materials', North Carolina State University, 1983.
8. Rowe, P.W., "The Stress-Dilatancy Relation for Static Equilibrium of an Assembly of Particles in Contact," Proc. of Royal Society A. 269, 1963, pp. 500~527.
9. Broese van Groenou, A. and Lissenburg, R.C.D., "Inhomogeneous Density in Die Compaction: Experiments and Finite Element Calculations," Communications of the Am. Ceramic Soc., Sept., 1983, pp. C 156~C158.
10. Broese van Groenou, A. and Knaapen, A.C., "Density variations in Die-compacted powders," Proc. of the 10 th International Conference on Science of Ceramics, Edited by Hausner, H., Sci. Ceram. 10, erchtesgaden, 1979, pp. 93~99.
11. Hehenberger, M., Samuelson, P., Alm, O., Nilsson, L., and Olofsson, T., "Experimental and Theoretical Studies of Powder Compaction," IUTAM Conference on Deformation and Failure of Granular Materials, Vermeer, P.A. and Luger, H.J., Ed., Delft, 1982, pp. 381~390.
12. Hehenberger, M. and Crawford, J.E.., "A Predictor Method for Finite Element Analysis of Sliding Friction," Scand. J. Metallurgy 12, 1983, pp. 285~288.
13. Thompson, R.A., "Mechenics of Powder Pressing: I. Model for Powder Densification," Am. Ceramic Society Bull. 60, pp. 237~243.
14. Thompson, R.A., "Mechanics of Powder Pressing: II. Finite Element Analysis of End-Capping in Pressed Green Powders," Am. Ceramic Society Bull. 60, 1981, pp. 244~247.

(접수일자 1987. 9. 1)